UV Raman Spectroscopy of H₂-Air Flames Excited with a Narrowband KrF Laser

John A. Shirley

United Technologies Research Center, East Hartford, CT 06108, USA

Abstract. Raman spectra of H_2 and H_2O in flames excited by a *narrowband* KrF excimer laser are reported. Observations are made over a porous-plug, flat-flame burner reacting H_2 in air, fuel-rich with nitrogen dilution to control the temperature, and with a H_2 diffusion flame. Measurements made from UV Raman spectra show good agreement with measurements made by other means, both for gas temperature and relative major species concentrations. Laser-induced fluorescence interferences arising from OH and O_2 are observed in emission near the Raman spectra. These interferences do not preclude Raman measurements, however.

Excimer lasers make available high pulse energies and repetition frequencies, potentially affording an attractive source of excitation for spontaneous Raman scattering measurements in combustion environments. With unstable resonators, high beam quality and efficient cavity extraction can be achieved. The short wavelength increases the Raman scattering cross section through the λ_s^{-4} dependence on the scattering wavelength, λ_s. In this regard, based on scattered energies, an excimer laser possessing 0.2 J of energy per pulse at 248 nm is equivalent to 7.5 J at 532 nm! In addition, the cross section is increased further, for molecules which absorb in the near UV, by resonant enhancement. Spontaneous Raman measurements are of interest for combustion diagnostics because temperature and all major species concentrations can be measured simultaneously. Although coherent anti-Stokes spectroscopy can be used for multiple species measurements [1], such approaches are in many ways more complex.

A nonintrusive, spatially-resolved method is desired to measure gas temperatures and species concentrations in the exhaust of rocket engines – specifically at the exit plane of the space shuttle main engine (SSME). The gas temperature ranges from 900 to 1400 K at the exit, and molecular hydrogen (24%) and water vapor (76%) are the major species.

Hargis [2] recognized the potential signal enhancement with an excimer laser and demonstrated the detection of nitrogen at 10^{-4} Torr pressure. Excimer lasers operating with broadband output also have been previously used for combustion measurements. Kobayashi et al. [3] reported the wavelength scaling of Raman cross sections for a number of molecules of interest in combustion using ArF (193 nm), KrF (248 nm), XeCl (308 nm), and XeF (351 nm) excimer lasers. They demonstrated an enhancement of the cross section for oxygen, due to near resonance, for wavelengths less than 290 nm and concluded that the KrF laser represented the most suitable excimer source for flame Raman spectroscopy. They also measured temperature from Stokes to anti-Stokes ratios, and carbon dioxide concentration profiles in a premixed methane-air flame. Pitz et al. [4] used broadband KrF and XeF lasers for spontaneous Raman measurements in H_2/air flames. They observed laser induced fluorescence (LIF) interferences, which they were unable to identify due to lack of spectral resolution.

Spontaneous Raman measurements in hydrogen-air combustion with a narrowband, tunable KrF laser are reported here. Narrowband operation is shown to be crucial to minimize interferences, which are unavoidable with broadband operation. These interferences arise from OH and O_2 laser induced fluorescence [5]. The measurement apparatus used for Raman measurements and the hydrogen flames are described next. The results of measurements are then reported and the identification of the source of LIF interferences is discussed. Finally, conclusions and recommendations for KrF laser excited Raman measurements are made.

1. Description of Apparatus

A commercial KrF laser (Lambda-Physik EMG-160T-MSC) is used in the measurement system [6]. In this laser, the tunable oscillator output is seeded into an unstable resonator amplifier. Raman scattered radiation is collected in a back-scattering configuration to utilize the predominantly horizontally polarized output of the laser. A cylindrical lens focuses the laser beam to an area approximately 100 µm by 8 mm. The focussed beam dimensions were measured from burn patterns on exposed photographic paper. The horizontal focal area of the laser is rotated in a periscope to align with the vertical spectrometer slit. For detection, the 0.5 m spectrometer is equipped with either a photomultiplier and gated integrator or a diode array. The sample volume viewed by the spectrograph is approximately 1 mm long, 15 µm high and 75 µm wide. Modification of the collection geometry would permit more efficient signal collection. The laser energy is 0.2 J per pulse. Diode array spectra shown later represent an accumulation of some 1000–2000 laser pulses.

The porous-plug burner is operated premixed with a mixture of hydrogen, air and nitrogen. Gas flow rates, measured with calibrated flowmeters, are adjusted to make the flame fuel-rich, with either 4 or 8% unburned hydrogen remaining in the post-flame gases. The excess nitrogen is added to the flow to maintain post-combustion gas at a temperature calculated [7] at 1400 K, assuming adiabatic flow, so as to simulate conditions in the SSME exhaust. The gas temperature was measured with a 3 mm diameter Pt–Pt 10% Rh thermocouple coated with $BeO-Yt_2O_3$. The measured gas temperature after applying a correction for radiation is 1180 K. Spectra typically are measured 19 mm above the burner surface, i.e. in the post-flame region.

2. Raman Measurements

Figure 1 shows a spectrum spanning a 10 nm wavelength range, including both H_2 and H_2O Raman Q-branches, with bandheads at 4155 and 3752 cm^{-1}, respectively. Individual components of the H_2 Q-branch near 277.2 nm are resolved and some structure is discernible in the H_2O spectrum with a bandhead at 273.4 nm.

A series of other peaks is also apparent at this particular laser frequency. These peaks have been identified as LIF from P, Q, and R transitions of hydroxyl radical. Excitation of OH LIF following absorption of KrF laser radiation in the $A^2\Sigma-X^2\Pi$ (3,0) band was described by Andresen et al. [5], who found fifteen absorption lines within the nominal tuning range of 40 190 to 40 320 cm^{-1}. The emission lines, arising from transitions within the (3,1) vibrational band, are labeled in Fig. 1. The transitions are connected to the $N = 11$ level of $A^2\Sigma(v' = 3)$ which is populated by the (3,0)Q_1(11) absorption at 248.352 nm [5]. The laser is tuned to a position near the center of the tuning range. The wavelength of the laser has been determined by calibrating the spectra with a neon lamp in first order; Raman spectra are recorded in second order. The Raman shift and measured wavelength of Q(3) of H_2 are then used to calculate the laser wavelength; which, in this case, is determined to be 248.35 nm (vacuum). This agrees very well with the wavelength of the absorbing Q_1(11) transition.

Figure 2 shows another laser tuning which excites a different triad of transitions corresponding to absorption by (3,0)P_2(8) at 248.457 nm. The Raman spectra are the same, but shifted in wavelength. Determining the laser wavelength, as before, gives 248.47 nm – in satisfactory agreement with the known absorption wavelength.
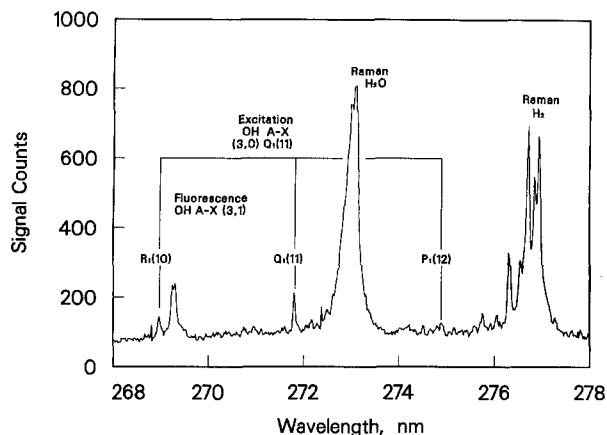

Fig. 1. Spectrum of H_2 and H_2O in H_2-air-N_2 flame. LIF from triplet of OH excited is identified. The laser wavelength is 248.35 nm
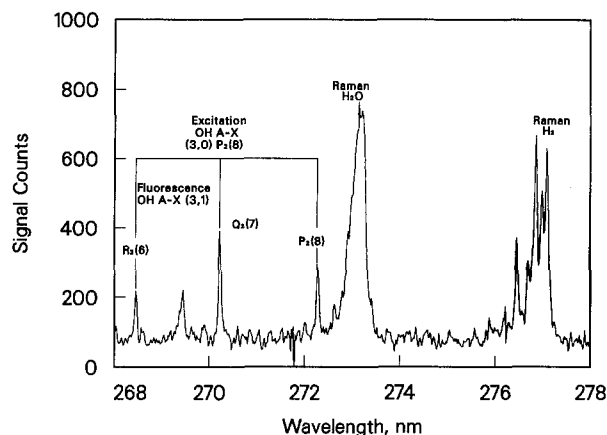

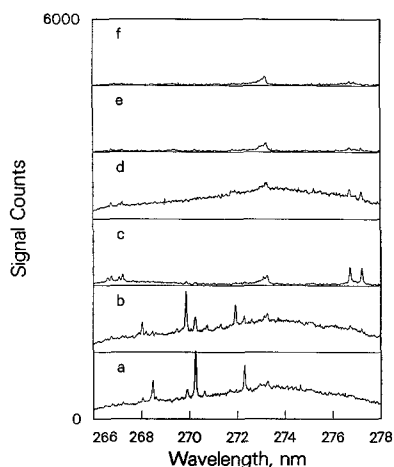**Fig. 2.** Spectrum of H_2 and H_2O Raman signatures and OH LIF with laser tuned to 248.47 nm

Fig. 3. The effect of tuning on spectra in the H_2 and H_2O Raman Q-branch wavelength region. The laser is tuned in 1.68 cm^{-1} steps between the spectra

Laser induced fluorescence interferences depend on the tuning of the laser with respect to absorbing species resonances. The dramatic effect of tuning is shown in Fig. 3, which presents a series of spectra at different laser frequencies separated by 1.68 cm^{-1}. These spectra were obtained in a small H_2-air diffusion flame. First, note the

Raman Q-branch of H_2O at 273.3 nm seen in all spectra. Hydrogen would be at 277.1 nm were it not consumed at the measurement point in the flame. The strong triads of transitions in a and b are OH transitions. The absorbing transition in a is $P_2(8)$ which pumps the level radiating into $P_2(8)$, $Q_2(7)$, and $R_2(6)$. Spectrum b shows transitions excited by absorption on the satellite transition $P_{12}(8)$, which then radiates to $P_1(8)$, $Q_1(7)$, and $R_1(6)$. c and d show oxygen LIF P and R transitions [5] excited by absorption on 0,6 and 2,7 vibrational bands of the Schumann-Runge band. The oxygen fluorescence lies at 266.3–268.8 nm for v', $v'' = 0,8$ and 2,9 vibrational bands, and 276.3–278.4 nm for 0,9 and 2,10 bands. The latter bands interfere with H_2 Raman, when combustion is incomplete. Spectra e and f show water vapor Raman spectra that are relatively free of LIF interferences.

The Raman Q-branch of hydrogen, measured in the premixed flame, is shown by the solid line Fig. 4. The dashed line is a calculation for 1200 K, appropriate to the thermocouple measured gas temperature. An instrument function for the spectrograph/OMA combination has been included in the calculation. The instrument function was determined independently by fitting the profiles of a number of well separated lines of a standard spectral lamp. The instrument function is dominated by the OMA detector (intensified diode array). The response profile consists of the combination of a sharp spike and a broad peak which is about 15% of the height of the spike and 4 times broader. Mathematically, the instrument function is fit with a double gaussian.

The accuracy of relative concentrations determined from UV Raman has been checked by comparison to the known reactant flowrates in the premixed flame. The species i population density, n_i is related to the signal count, N_R, integrated across the Raman band:

$$N_R = \frac{E_L \sigma_i n_i l \Omega \varepsilon}{hck_i^S},$$ (1)

where E_L is the incident laser energy, σ_i is the Raman cross section, l is the length of the scattering volume, Ω is the collection solid angle and ε is the counting efficiency, which combines collection efficiency and detector efficiency. k_i^S is the Stokes-shifted energy of the photon

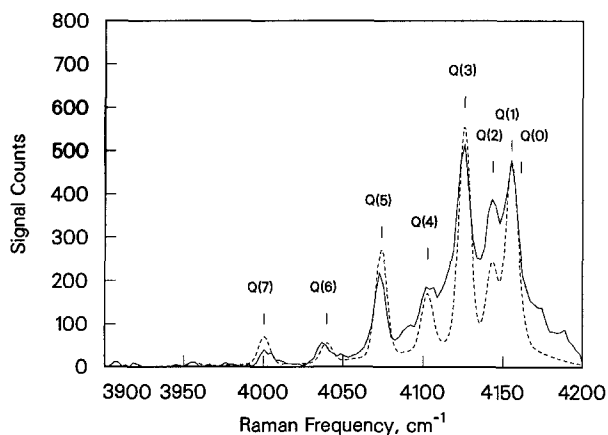scattered by species i and h and c are Planck's constant and the speed of light respectively. The relative H_2 and H_2O densities can be expressed as

$$\frac{n(H_2)}{n(H_2O)} = \frac{\sigma/k_s(H_2O)}{\sigma/k_s(H_2)} \frac{N_R(H_2)}{N_R(H_2O)}.$$ (2)

The ratio of the Raman cross sections is the most uncertain quantity in this expression. The range of literature values [8, 9] for the ratio $\sigma(H_2)/\sigma(H_2O)$ is 0.92–1.1, with stated accuracies of 10%. The uncertainty in the measured Raman counts is estimated to be about 7%.

The measured ratio $N_R(H_2)/N_R(H_2O) = 0.76 \pm 0.05$ as determined from spectra shown in Figs. 1 and 2. Therefore the ratio of concentrations: $n(H_2)/n(H_2O) = 0.69 \pm 0.11$, measured in the post-flame gas. This ratio implies a fuel equivalence ratio, $\phi = 1.69 \pm 0.11$ which agrees within experimental error with the equivalence ratio determined by the gas flowmeters: $\phi = 1.60$.

3. Laser-Induced Fluorescence Interferences

The origin of the OH species observed in laser induced fluorescence is of interest. One source is flame chemistry, but KrF laser radiation is also known to produce OH by two-photon photodissociation of water vapor [10, 11]. Ninety percent of the OH produced this way is in the ground electronic state. The remaining 10% is found in either $v' = 0$, or $v' = 1$ of the $A^2\Sigma$ state [10]. If the OH arises from two-photon photodissociation, the laser-induced fluorescence nominally should scale as the square of the laser power. In the post-flame zone of the premixed flame, the measured OH LIF level relative to the (linear) Raman scattering remained constant when the power was reduced by one-half, supporting the flame chemistry as the origin of OH in these measurements.

The effect of laser energy on OH LIF has also been studied in the small H_2 diffusion flame. This flame is hotter, so higher OH levels are expected. Figure 5 shows the OH LIF signal for connected P, Q, and R transitions measured as a function of laser energy. A small departure from linearity is present. A two level model was assumed in calculations to simulate the temporal behavior of OH
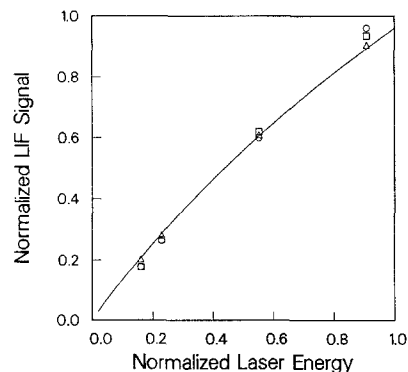

Fig. 4. Raman spectrum of H_2 Q-branch in H_2-air-N_2 fuel-rich flame described in the text (solid line). The dashed line shows a spectrum calculated for a 1200 K temperature flame

Fig. 5. Dependence of OH LIF P, Q, and R signals on KrF laser pulse energy. The solid line is the calculation discussed in the text

levels pumped by UV radiation and to evaluate this measurement. The equations for the time dependence of the upper ($v' = 3$) and lower ($v'' = 0$) OH levels, N_2 and N_1 respectively are [12]:

$$\frac{dN_1}{dt} = -N_1 \frac{B_{12}}{c} I + N_2 \left(\frac{g_1}{g_2} \frac{B_{12}}{c} I + A_{21} + Q_{21} \right), \qquad (3)$$

$$\frac{dN_2}{dt} = N_1 \frac{B_{12}}{c} I - N_2 \left(\frac{g_1}{g_2} \frac{B_{12}}{c} I + A_{21} + Q_{21} P_2 \right), \qquad (4)$$

where B_{ij} is the Einstein coefficient for stimulated emission, I is the laser spectral intensity, A is the Einstein coefficient for spontaneous emission, and Q and P are respectively the rates for quenching and predissociation. For these calculations $N_2 + N_1 \neq \text{const}$ because of the predissociation term. Key data for the $v = 3$ level are not well known for OH. Andresen et al. [5] estimated a predissociation lifetime of 100 ps from the amount of rotational energy transfer evident in their OH LIF spectra. Sink et al. [13] have calculated predissociation linewidths for a number of vibrational levels. The radiative transition rates for many vibrational-rotational levels of OH have been calculated by Chidsey and Crosley [14] but values for the levels of interest here are not included. The predissociation and quenching rates are the more important parameters. In the calculations herein: $I = 4.5 \times 10^9$ W/cm at the maximum, $P = 10^{10}$ s^{-1} and $B = 2.5 \times 10^{11}$ cm^2/J-s. The model calculations, which include a gaussian temporal laser pulse indicate that predissociation dominates the loss mechanisms and determines the temporal evolution of the radiation driven populations. The LIF signal level, calculated as a function of laser spectral intensity, is shown by the solid line in Fig. 5. The calculations represent the data quite well, supporting the hypothesis of a flame chemistry source for the OH, as might be expected in this flame, and also indicate the onset of saturation.

All of the main OH branch transitions: 3-1, 3-2, and 3-3 bands, which fluoresce from the laser prepared $A^2\Sigma$ state, do so at wavelengths that do not interfere seriously with either H_2 or H_2O Raman spectra with only one exception. Absorption at the $A-X$ 3,0 $R_1(15)$ transition at 248.48 nm results in fluorescence from 3,1 $Q_1(16)$ at 275.54 nm [14] which is close to the $Q(7)$ Raman transition of H_2. With excitation at the $R_1(15)$ wavelength, the H_2 $Q(7)$ transition appears at 275.91 nm. However, the fractional population in $N = 15$ is small for the relatively low temperature flames investigated here. For example, at 1200 K the population in the level absorbing $R_1(15)$ is more than an order of magnitude less than the population in the level absorbing $P_2(8)$. This makes the $R_1(15)$ difficult to observe, as was confirmed by the experiments. At 2000 K the population ratio $n(N = 15)/n(N = 8)$ is about 0.2, so $R_1(15)$ becomes a more important potential interference in hotter flames. There are also several satellite branch transitions [15] radiating at wavelengths throughout the H_2 Q-branch, but the linestrengths of these are typically only 2% of the main transitions and at most 10% for low rotational levels. Therefore, for measurement near the flame front, where OH interferences are a concern, it is prudent perhaps to avoid the 3,0 $R_1(15)$ transition by suitably tuning the laser. On the other hand, measurements with a *broadband* KrF laser would excite all these transitions and entail degraded Raman signal-to-noise ratios because of the LIF interferences.

O_2 LIF can interfere with H_2 Raman in unburned flame zones, where O_2 and H_2 concentrations are high. For Raman measurements, the laser frequency should be chosen to avoid all these interferences, to the extent possible. Several windows exist in the excitation spectra of OH and O_2 in the KrF laser tuning range. A laser frequency near 40 255 cm^{-1} avoids proximity to the OH and O_2 absorption and is close to the center of the KrF tuning range.

4. Conclusions

The LIF interference levels observed here do not preclude analysis of the Raman spectra for temperature or concentrations as demonstrated. Account would need to be made of the presence of LIF for accurate measurements. OH concentrations could be deduced from spectra in cases where the predissociation rates are known and exceed quenching rates. In a broader range of combustion applications, the relative strength of OH interferences could vary widely, particularly in hotter flames. The source of OH has been shown, for these measurements, to be combustion chemistry, rather than two-photon photodissociation of water vapor. While it should be possible to tune the narrowband KrF laser to avoid these interferences, high injection locking efficiency will be an important requirement to achieve Raman spectra free of interferences.

References

1. A.C. Eckbreth, T.J. Anderson: Appl. Opt. **24**, 2731 (1985)
2. P.J. Hargis, Jr.: Appl. Opt. **20**, 129 (1981)
3. T. Kobayashi, M. Konishi, M. Ohtaka, S. Taki, M. Ueda, K. Kagawa, H. Inaba: In *Laser Diagnostics and Modeling Combustion*, ed. by K. Iinuma, T. Asanuma, T. Ohsawa, S. Taki (Springer, Berlin, Heidelberg 1987) p. 133
4. R.W. Pitz, J.A. Wehrmeyer, J.M. Bowling, T.S. Cheng: Presented at Central States Combustion Institute meeting in Indianapolis, May, 1988
5. P. Andresen, A. Bath, W. Gröger, H.W. Lülf, G. Meijer, J.J. ter Meulen: Appl. Opt. **27**, 365 (1988)
6. J.A. Shirley, L.R. Boedeker: AIAA Paper 88-3038 (1988)
7. S. Gordon, B.J. McBride: NASA Report SP-37 (1971)
8. J.M. Cherlow, S.P.S. Porto: "Laser Spectroscopy of Gases" in *Laser Spectroscopy of Atoms and Molecules*, ed. by H. Walther (Springer, Berlin, Heidelberg 1976)
9. H. Inaba, T. Kobayasi: Opto-Electronics **4**, 101 (1972)
10. G. Meijer, J.J. ter Meulen, P. Andresen, A. Bath: J. Chem. Phys. **85**, 6914 (1986)
11. C. Fotakis, C.B. McKendrick, R.J. Donovan: Chem. Phys. Lett. **80**, 598 (1981)
12. R.P. Lucht: "Applications of Laser-Induced Fluorescence for Combustion and Plasma Diagnostics" in *Laser Spectroscopy and Its Applications* ed. by L.J. Radziemski, R.W. Solarz, J.M. Paisner (Dekker, New York 1987)
13. M.L. Sink, A.D. Bandrauk, R. Lefebvre: J. Chem. Phys. **73**, 4451 (1980)
14. I.L. Chidsey, D.R. Crosley: J. Quant. Spectrosc. Radiat. Transfer **23**, 187 (1980) and reference 13 therein
15. G.H. Dieke, H.M. Crosswhite: J. Quant. Spectrosc. Radiat. Transfer **2**, 97 (1962)